Mechanistic insight into heterogeneity of trans-plasma membrane electron transport in cancer cell types

Harry G. Sherman[a], Carolyn Jovanovic[b], Alaa Abuawad[c], Dong-Hyun Kim[c], Hilary Collins[d], James E. Dixon[a], Robert Cavanagh[e], Robert Markus[f], Snow Stolnik[e], Frankie J. Rawson[a],*

[a] *Division of Regenerative Medicine and Cellular Therapies, School of Pharmacy, University of Nottingham, Nottingham NG7 2RD, United Kingdom*
[b] *Walgreens Boots Alliance, Nottingham NG2 3AA, United Kingdom*
[c] *Division of Advanced Materials and Health Technologies, School of Pharmacy, University of Nottingham, NG7 2RD, United Kingdom*
[d] *Division of Biomolecular Science and Medicinal Chemistry, School of Pharmacy, University of Nottingham, Nottingham NG7 2RD, United Kingdom*
[e] *Division of Molecular Therapeutics and Formulation, School of Pharmacy, University of Nottingham, Nottingham NG7 2RD, United Kingdom*
[f] *SLIM Imaging Unit, Faculty of Medicine and Health Sciences, School of Life Sciences, University of Nottingham, Nottingham NG7 2RD, United Kingdom*

ABSTRACT

Trans-plasma membrane electron transfer (tMPET) is a process by which reducing equivalents, either electrons or reductants like ascorbic acid, are exported to the extracellular environment by the cell. TPMET is involved in a number of physiological process and has been hypothesised to play a role in the redox regulation of cancer metabolism. Here, we use a new electrochemical assay to elucidate the 'preference' of cancer cells for different trans tPMET systems. This aids in proving a biochemical framework for the understanding of tPMET role, and for the development of novel tPMET-targeting therapeutics. We have delineated the mechanism of tPMET in 3 lung cancer cell models to show that the external electron transfer is orchestrated by ascorbate mediated shuttling *via* tPMET. In addition, the cells employ a different, non-shuttling-based mechanism based on direct electron transfer *via* Dcytb. Results from our investigations indicate that tPMETs are used differently, depending on the cell type. The data generated indicates that tPMETs may play a fundamental role in facilitation of energy reprogramming in malignant cells, whereby tPMETs are utilised to supply the necessary energy requirement when mitochondrial stress occurs. Our findings instruct a deeper understanding of tPMET systems, and show how different cancer cells may preferentially use distinguishable tPMET systems for cellular electron transfer processes.

1. Introduction

Trans-plasma membrane electron transport systems (tPMETs) transport electrons across the cell plasma membrane. These systems are expressed in cells across all forms of life [1]. They are understood to be involved in a range of physiological processes [2], including protection from external oxidants [3,4], defence against infection [5,6], the maintenance of intracellular redox state [7], iron reduction [8–10], sperm maturation and fertilisation [11–13], and platelet activation [14–16]. TPMET is further hypothesised to play a role in cancer energy metabolism [17–19]. Otto Warburg first suggested the reprogramming of energy metabolism to a state of aerobic glycolysis as a fundamental change of the cancer cell phenotype [20]. This reprogramming of energy metabolism is now thought of as a hallmark of cancer [21,22]. One result of a preferential use of aerobic glycolysis would be an increase in reduced nicotinamide adenine dinucleotide (NADH), due to less oxidative phosphorylation to convert NADH to NAD^+. TPMET may play a role in cancer biogenesis by maximising the levels of NAD^+ regeneration, and this would allow the facilitation of greater metabolic flux *via* glycolysis, thereby alleviating cellular stress [3,17,18,23,24]. The pentose phosphate pathway is also upregulated in cancer [25], which is linked to tPMET through nicotinamide adenine dinucleotide phosphate (NADPH) electron donation, and ascorbate regeneration using glutathione (GSH) and NAD(P)H [26]. It is important to note that this role is not fully elucidated, and more studies are required to investigate this further.

In the intestinal and pulmonary epithelium tPMET has been reported to be involved in the transport of metals [8,27]. The mechanisms of this apical membrane electron transport in the lung and intestine are thought to be similar, and can occur *via* an enzyme mediated process, of

---

* Corresponding author.
  E-mail address: frankie.rawson@nottingham.ac.uk (F.J. Rawson).

which duodenal cytochrome *b*561 (Dcytb) has been suggested as a mediator [9], or alternatively *via* a cross membrane ascorbic acid (vitamin C, ascorbate) shuttle system. Both systems reduce apical ferric iron to ferrous iron, thus enabling its transport across plasma membrane *via* transporters such as the divalent metal transporter 1 [27,28] (DMT1). The ascorbate shuttling mechanism of tPMET has been shown to occur in K562 leukaemia cells [29], skeletal muscle cells [30], astrocytes [31], monocytes [32], and Caco-2 cells [33]. There is also a substantial body of research into solely ascorbate shuttling – not involving the reduction of an external electron acceptor - in human cells, including in astrocytes [34,35], endothelial cells [36,37], hepatocytes [38], and neuroblastoma cells [39]. Some research has also been conducted into the release of ascorbate and its presence the lung in guinea pigs, rats, and in human lung lavage [40–42]. It has also been reported that Iron uptake by human bronchial epithelial cells uses tPMET that can involve Dcytb [9].

Studying tPMET systems is important as they are currently implicated as a potential targets to inducing anti-proliferative effect in cells *in vitro* [19,43]. The research reported by Grasso et al. [19] and Prata et al. [43] used ubiquinone-based compounds targeting tPMET to produce anti-leukemic activity, in combination with intracellular redox disruption. Ruthenium-based compounds have also been investigated for similar purpose [44], whilst cancer therapy using pharmacological doses of ascorbate is a rapidly growing approach [45–49].

The presence of cell-surface oxidoreductase systems is well known [50], and there is mounting evidence that tPMET systems can facilitate the re-oxidation of intracellular NAD(P)H, in response to decreased mitochondrial activity, in various cell types [7,17,18,51]. Where the current understanding will benefit is the integration of how both shuttle and enzyme-based tPMET systems are used in tandem, and the differences in their utilisation between different cell types. This would mean that efforts to target tPMET activity in cancer need to consider the differences in the use of these systems by different cancer cell types, if tPMET is to be used as a target for cancer therapy.

Recent work *in vivo* has suggested that cancer cells reduce ascorbate levels to increase expression of the hypoxia-induced factor 1 (HIF1), but still maintain levels of ascorbate at 60–70% of 'normal' physiological level [52]. It was also suggested that this is due to a higher turnover of ascorbate in tumorigenic cells [47].

We focus our work on cells of epithelial origin from the lung, as previous work found that iron-related tPMET systems are active in the lung and intestine epithelial tissues. This would mean that in these cells the necessary mechanisms for tPMET regeneration of intracellular redox couples are already present and active. The activity is primarily attributed to exposure to high levels of catalytically active iron and the need for its detoxification [8].

Regeneration of ascorbate from either dehydroascorbate (DHA) or the ascorbate free radical (AFR) can occur in several ways [26]. Reduction of dehydroascorbate (DHA) to ascorbate can be facilitated inside of the cytosol by direct non-enzymatic reduction *via* glutathione [53]; by the NADPH-dependant enzymes thioredoxin reductase [54] or 3-alpha-Hydroxysteroid dehydrogenase [55]; or through the gluthathione-dependant enzymes glutaredoxin [56], protein sulphide disomerase [56] and omega class glutathione transferase [57]. The free radical of ascorbate (AFR), can be reduced to ascorbate either in the cell *via* NADPH-dependant thioredoxin reductase [58] or NADH-dependant cytochrome *b*₅ reductase [59], and can be regenerated extracellularly *via* a cell surface NADH:AFR reductase [60]. Since DHA and the AFR are reduced using mechanisms utilising NAD(P)H and glutathione (GSH), this forms an interplay with the glycolytic and pentose pathways of the cell.

In this work we aim to delineate the biochemical systems that occur in tPMET in selected malignant lung epithelium. The work expands on current knowledge on interplay of different tPMET processes, the potential role of tPMET in cancer, and the ability of varying cell types to use differing mechanisms to achieve tPMET. The work builds on our

recent report on differences in electrical charge flux that exist in different types of epithelial cancer cells originating from the lung tissue [61].

We used a newly developed electrochemical method [61] – in corroboration with lactate spent medium analysis to establish basal level tPMET activity in the cancer cell models. In combination with chemical inhibitor and knock down studies two tPMET systems were identified. One charge transfer mechanism occurred *via* an ascorbate shuttle tPMET. The second was *via* a Dcytb redox protein based tPMET. We also provide evidence based on cell metabolism, viability and mitochondrial function that tPMET activity could be linked to energy reprogramming of cancer cells.

2. Methods

2.1. Materials

All materials were supplied by Sigma Aldrich Ltd., unless otherwise stated.

2.2. Cell culture

The three cell lines tested in this study were Calu-3, H1299, and A549. Calu-3 cells (ATCC® HTB-55) are a human lung adenocarcinoma derived from a pleural effusion metastatic site of the bronchial lung epithelium, and of epithelial type. H1299 cells (ATCC® CRL-5803™) are non-small cell human lung adenocarcinoma cells derived from a lymph node metastatic site of the lung, and of epithelial type. A549 cells are non-small cell adenocarcinomic human alveolar (type II) basal epithelial cells, and are commonly used as an alveolar type II model. All cell lines were purchased from American Type Culture Collection (ATCC).The passage numbers for all the experiments were between 32 and 37 for Calu-3 cells, 10–21 for H1299 cells, and 11–24 for A549 cells. Any detachment of cells was performed by 0.5 mL 0.25% trypsin/EDTA (with phenol red). All cells were grown in DMEM (Dulbecco's Modified Eagles Medium) containing high glucose supplemented with 10% *v/v* FBS (fetal bovine serum), 100 U/mL penicillin, 100 μg/mL streptomycin, and 24 mM HEPES (N-(2-hydroxyethyl) piperazine-N′-(2-ethanesulfonic acid)) buffer at 37 °C, 5% CO_2. For all experiments Calu-3 cells were harvested after 4 days, and A549 and H1299 cells following 3 days of growth. This ensured all three cell lines were in an exponential growth phase when used in experiments, as described previously [61]. All cells were harvested at a confluency of ~90%. Unless otherwise stated, following the growth period the medium was aspirated, and cells washed three times with warm phosphate buffered saline (PBS). All cell assays were performed at 37 °C and with supplemented media unless otherwise stated. For all experiments performed in a 6 well format wells contained, g 6.3×10^5 cells/well for Calu-3 cells, and 2.5×10^5 cells/well for A549 and H1299 cells, unless described otherwise. Cell counting and trypan blue exclusion assays were performed on all cell assays.

2.3. Electrochemical analysis

A three-electrode system comprising a 33 μm carbon fibre working microdisk electrode, a saturated calomel reference electrode, and a platinum wire counter electrode was used for all electrochemical analysis (ALS Co. Ltd., Japan). An Autolab PGStat302A potentiostat with low current detection module (ECD) (Metrohm Autolab, Utrecht, Netherlands) and NOVA 2.1 software was used in all experiments. Linear sweep voltammetry was performed with solutions containing differing ratios of oxidised and reduced forms of iron (as above) and were carried out by scanning from 650 to −150 mV, at a scan rate of 10 mV s⁻¹. A current range of 100 pA was used for all experiments, with a low current module employed for all experiments. All electrochemistry was recorded with a HBSS only sample acting as a control to

allow for baseline subtraction. Between each solution tested, the microelectrode was polished for 4 min using a PK-3 electrode polishing kit (ALS Co. Ltd., Japan). Pseudo steady-state values were determined by assessing a first derivative function of the voltammogram and cross-referencing with the original curve to clarify that this was the voltage where the pseudo steady state was located.

2.4. Ascorbic acid 'loading' and determination of intracellular ascorbic acid concentrations

Calu-3 cells were added to give 2.5×10^4, and H1299 and A549 at 1.0×10^4 cells per well in 2 mL of DMEM in a 12 well plate. The cells were incubated for 30 min with either 0, 250, 500, 750 or 1000 μM dehydroascorbic acid (DHA) in phosphate buffered saline (PBS, 0.01 M, pH 7) for 30 min. Determination of intracellular ascorbic acid concentration was conducted according to a the ferrocyanide determination assay of Lane and Lawen [62]. After incubation, the solution was aspirated, and the cells washed three times in warm (37 °C) PBS. Cell suspensions were centrifuged at $250 \times g$ for 5 min, re-suspended in ice-cold PBS, and then centrifuged for the second time at $250 \times g$ for 5 min. Aspiration of the PBS resulted in cellular pellet. The cell pellet was re-suspended in 0.1% (w/v) saponin solution in ice-cold PBS and agitated on ice for 10 min to ensure thorough cellular lysis. Cellular debris was removed by centrifugation of the crude lysate at $16,000 \times g$ for 5 min in a refrigerated microcentrifuge (4 °C). 100 μL aliquots from each sample were added to wells in a 96-well flat bottom plate that contained either 25 μL/well of PBS without L-ascorbate-oxidase (AO) or 25 μL/well of 45.5 U/mL stock solution of AO in PBS. A set of standards of 0, 2.5, 5, 10, 15 and 20 μm of L-ascorbic acid were also prepared and added to wells with or without AO, as above. The 96 well plate was left at room temperature for 5 min in the dark, followed by the addition of 3.5 mM potassium ferricyanide (FIC) in PBS to all wells. The plate was further incubated at room temperature in the dark for 5 min, before the addition of 25 μL of a freshly constructed solution containing 50% (v/v) acetic acid and 30% (w/v) trichloroacetic acid (TCA) to all wells. Immediately afterwards the following solutions were added to all wells: 100 μL of a ferrocyanide (FOC) determination solution containing 2 mL of 3 M Na-acetate (pH 6.0), 0.5 mL of glacial acetic acid (~17.4 M acetic acid), 2 mL of 0.2 M citric acid, 2 mL of 3.3 mM FeCl₃ in 0.1 M acetic acid, and 1 mL of 30 mM ferene-S. The plate was incubated for 30 min in the dark at room temperature. Absorbance was read at 593 nm using a Tecan plate reader (Spark 10 M, Tecan Ltd). The amount of intracellular ascorbate as nmole ascorbate per cell was calculated by initially subtracting the absorbance values at $\lambda_{593\ nm}$ for the '+ AO' wells from the corresponding '- AO' wells for each of the standard samples, and plotting a standard curve of the known concentration against the $\lambda_{593\ nm}$. The difference between AO positive '+ AO' and AO negative '-AO' wells was plotted for each of the cellular samples, and the quantity of ascorbate obtained interpolated from the standard curve. This experiment was carried out with two technical repeats and four biological repeats.

2.5. MTS cell assay

The MTS (3-(4,5-dimethylthiazol-2-yl)-5-(3-carboxymethoxyphenyl)-2-(4-sulfophenyl)-2H tetrazolium) assay (CellTiter 96, Promega) in 96-well plate format was used to test the mitochondrial metabolic activity of the cells incubated with DHA (ascorbic acid 'loaded'). Cells were added to give 8.4×10^3 cells per well for A549, and H1299, and 2.1×10^4 cells per well for Calu-3 cells in 150 μL of DMEM in 96 well-plate. The cells were incubated with 0, 100, 200, 300, 400, 500, 600, 700, 800, 900 and 1000 μM of DHA in PBS for 30 min. Following incubation, cells were washed once with warm PBS and incubated with 20.0 μL of MTS reagent in 100 μL of DMEM (without antibiotics) per well for 2 h. Blank subtractions consisted of DMEM without antibiotics. Relative metabolic activity was calculated by

setting the absorbance, measured at $\lambda_{490\ nm}$ for the untreated cell control as 100%, and the positive control (0.2% v/v Triton X-100 solution) was assumed to result in total cell lysis and set at 0%. This experiment was carried out with three technical repeats and three biological repeats.

2.6. Inhibition of GLUT1-mediated DHA uptake

A549 and H1299 cells were added to give 0.10×10^6 cells/well, and Calu-3 cells at 0.25×10^6 cells/well in 12 well plates. The cells were incubated with either 0 μM DHA solution, 750 μM DHA solution, or 750 μM DHA and 50 μM cytochalasin B (CB) solution, all prepared in PBS for 30 min. Following the incubation intracellular ascorbic acid levels were determined by Lane and Lawen [62] assay as described above. This experiment was carried out with two technical repeats and three biological repeats.

2.7. Bicinchoninic acid assay

Following the removal of the cell incubation medium for electrochemical analysis of cell conditioned samples, wells were washed three times with PBS by gentle swirling for 5 min. 1.0 mL of 2% Triton X-100 solution in PBS buffer was then added to each well and the plates incubated 20 min. The lysed cell samples were then transferred to a micro-centrifuge tube and centrifuged at $16000 \times g$ for 20 min. The supernatant was removed and transferred to a fresh micro-centrifuge tube before analysis using a Pierce™ BCA Protein Assay Kit (ThermoFisher Scientific Ltd) using the manufacture's recommended protocol.

2.8. Anion channel inhibition

The cells for all three cell lines were added to a 6 well plate. To supplement ('load') cells with ascorbic acid, the cells were incubated with 750 μM dehydroascorbic acid (DHA) solution in PBS for 30 min at 37 °C. DHA solution was aspirated, the cells washed with PBS, and then incubated with 0 or 500 μM 4,4′-diisothiocyano-2,2′-stilbenedisulfonic acid (DIDS) in DMEM (no antibiotics), for 20 min. DIDS solution was aspirated and the cells washed with PBS. The cells were then incubated with HBSS for 45 min. An electrochemical assay was then performed as described above, with some modifications. In this instance 1.0 mL aliquots were taken from two wells, one with and one without DIDS, for electrochemical analysis. Electrochemical analysis was carried out as described under the 'electrochemical analysis' section, with concomitant bicinchoninic acid assay for protein quantification, also as described above. In a separate experiment the viability of the cells following this assay procedure was tested. The same protocol was followed until electrochemical analysis step, whereby instead of electrochemical analysis the cells were detached using EDTA. This experiment was carried out with one technical repeat, and five biological repeats.

Inhibition was carried out with two further inhibitors. The experiment was carried out as described in this section, with some modifications. Following seeding, culture and DHA incubation and removal (all as described above), the cells were incubated with 0 or 500 μM Disodium 4-acetamido-4′-isothiocyanato-stilben-2,2′-disulfonate (SITS) or 100 μM 5-Nitro-2-(3-phenylpropylamino)benzoic acid (NPPB) in DMEM not supplemented with FBS for 20 min. The inhibitor solution was aspirated and the cells washed. The cells were then incubated in HBSS for 45 min prior to the removal of 1 mL of supernatant. Electrochemical analysis was carried out on the supernatant as previously described in the 'electrochemical analysis' section. A concomitant bicinchoninic acid assay for protein quantification as described. This experiment with NPPB and SITS was carried out with three technical repeats and three biological repeats.

2.9. tPMET activity in cells not loaded with ascorbic acid

The cells were added to a 6 well plate. Either HBSS or 0.1 mM ferrocyanide (FIC) in HBSS was added. Following two hours incubation, 1.0 mL of culture medium was removed and tested electrochemically, as described in the electrochemical analysis method section. This experiment was carried out with three technical repeats and three biological repeats.

2.10. Metabolomics analysis of cell culture medium

The cells were added in 6 well plate. Cells were washed in PBS buffer and either DMEM, HBSS, 0.01 mM FIC in HBSS, or 0.1 mM FIC in HBSS was added to the wells and cells incubated for 2 h at 37 °C. 300 μL of DMEM was then removed and centrifuged at $3000 \times g$ for 5 min. 250 μL of the supernatant was transferred to a fresh tube containing 750 μL of pre-cooled (-20 °C) methanol. The solution was vortexed for 1 min to precipitate proteins. The precipitate and supernatant samples were then incubated at -20 °C for 20 min prior to vortexing for 15 s, and subsequent centrifugation at $12000 \times g$ for 10 min at 4 °C. The supernatant was collected and stored at -80 °C.

Preparation of the samples for metabolomics analysis consisted of placing 100 μL of each sample into pre-labelled auto-sampling tubes with 200 μL glass inserts. A quality control (QC) sample was also prepared containing an equal portion of all samples tested for instrument performance assessment [63]. Mass spectrometry analysis was carried out using an Orbitrap mass spectrometer (Thermo Exactive) in combination with liquid chromatography (LC) (Thermo Accela) from Thermo Scientific (Thermo Fisher Scientific, Hemel Hempstead, UK). It was operated with electrospray ionization (ESI) running in the negative (ESI-) and positive (ESI+) modes. The voltages used for the experiment were: spray voltage, 4500 V (ESI+) and 3500 V (ESI-), capillary voltage at 40 V (ESI+) and 30 V (ESI-), tube lens voltage at 70 V for both (ESI+) and (ESI-), skimmer voltage at 20 V (ESI+) and 18 V (ESI-). Sheath gas 40, desolvation gas 5, and sweep gas 1. The temperature for this experiment was maintained at 275 °C and 150 °C for capillary and probe, respectively. Mass calibration was carried out for both positive and negative mode before the analysis of each patch. The mass range was up to 1400 m/z for positive and negative modes, and the run time was 24 mins for each sample. To separate the components chromatographically a ZIC-pHILIC (4.6×150 mm and 5 μm particle size, Merck Sequant) was used. The mobile phase was composed of 20 mM ammonium carbonate in water (solvent A) and 100% acetonitrile (solvent B). Metabolites were separated according to a linear gradient as following: 0–15 min, 20% A, 15–17 min, 95% A, 17–24 min, 20% A at 300 μL/min flow rate and the injection volume of 10 μl. and the temperature of the column was kept at 45 °C.

To process raw data obtained from LC-MS, XCMS [64] and mzMatch [65] were used for untargeted peak-picking and peak matching, respectively. IDEOM was performed for putative metabolite identification and noise filtering based on default parameters [66]. Metabolite identification considered two levels of identification; level 1 (L1) identification according to the metabolomics standards initiative by matching retention times and accurate masses of authentic standards, and level 2 (L2) identification when the predicted retention times were employed as the standards were not available [67]. Pre-processed data were analysed statistically by performing multivariate and univariate analysis. Orthogonal partial least squares-discriminant analysis (OPLS-DA) was carried out by SIMCA-P v13.0.2 (Umetrics, Umea, Sweden) as a supervised multivariate model. This multivariate analysis was used as the first step for separation data into classes and evaluate the metabolic changes in HBSS, 0.01 FIC in HBSS or 0.1 mM FIC in HBSS treated cells for each cell line (Calu-3, A549 and H1299 cells). OPLS-DA was validated by the multiple correlation coefficient (R^2), and further cross-validated R^2 (Q^2) which is the predictability of the model. The key mass ions representing potential biomarkers were determined based on

Variable Importance in Projection (VIP) values obtained from two-way orthogonal comparisons. Mass ions with VIP values greater than one were considered as discriminant biomarkers. Univariate analysis was performed in parallel to multivariate analysis. t-test with false discovery rate (FDR) correction was performed using Metaboanalyst to find the significantly changed mass ions between HBSS, 0.01 FIC in HBSS or 0.1 mM FIC in HBSS treated cells for each cell line (Calu-3, A549 and H1299 cells). Mass ions with FDR < 0.05 and VIP > 1 were considered as statistically significant. MetaboAnalayst is a web server that afford metabolomic data analysis, interpretation and visualisation Kyoto Encyclopedia of Genes and Genomes (KEGG) database was used to analyse and visualize the affected pathway. This experiment was carried out with one technical repeats and six biological repeats.

2.11. Extracellular ascorbic acid as a component of tPMET

The cells were loaded with ascorbic acid, as described above, and then incubated in either HBSS, 0.1 mM FIC in HBSS, HBSS containing 10 U/mL AO, or HBSS containing 0.1 mM FIC and 10 U/mL AO, in triplicate. Following two hours incubation, 1.0 mL of cell medium was removed, and tested electrochemically, as described above. Values for 'HBSS samples' were subtracted from 'FIC samples' to remove any current contribution from the buffer in the voltammograms.

An electrochemical assay was performed in either HBSS, or 0.1 mM FIC in HBSS, in triplicate. An additional plate contained either HBSS + 10 U/mL AO, or 0.1 mM FIC + 10 U/mL AO added to the cells, in triplicate. Following two hours incubation, 1 mL of supernatant was removed, and tested electrochemically, as described above. HBSS incubated samples were subtracted from FIC samples to remove any current contribution from the buffer. The experiment was carried out in three technical repeats and four biological repeats.

2.12. Live cell immunofluorescence imaging

Cells were seeded in 24 well plates onto poly-L-lysine coated coverslips at 1.25×10^5 per well for Calu-3 cells, or 5×10^4 for H1299 and A549 cells and incubated for 24 h. The well plate was transferred onto ice for the duration of the experiment. Following each staining step the wells were washed three times by 5 min swirling with ice-cold PBS. Non-specific binding was blocked by incubation in 1.0% PBA (1% bovine serum albumin in PBS) for 30 min (500 μL). The plate was gently rocked during incubation. Primary antibody staining was carried out with anti-cytochrome b reductase 1 antibody (ab66048, Abcam Ltd) at 10 μg/mL in 1% PBA for 1 h. Secondary staining with donkey anti-rabbit IgG (H + L) Highly Cross-Adsorbed, Alexa Fluor® 647 (ThermoFisher Scientific Ltd., A31573) was carried out at 2 μg/mL for 45 min in the dark. Following secondary antibody staining, two drops of NucBlue™ Live ReadyProbes™ Reagent (ThermoFisher Scientific Ltd) was added to all wells.

Imaging of live cell samples was carried out using Zeiss PS1 Super Resolution Microscope with a 63× water lens. The far red channel (633 nm laser line) for Dcytb staining (displayed as red) used a gain of 750 and a laser power of 10%, whilst the blue channel (488 nm laser line) used a gain of 800 and a laser power of 4%. Z-stack slice and 3D images were analysed using Zen Black (Zen Software Ltd). Images were taken of multiple areas to confirm staining was representative of the cell population.

2.13. Transfection protocol

Pre-constructed plasmids were ordered from SigmaAldrich Ltd. Control plasmid: MISSION® pLKO.1-puro TurboGFP™ shRNA Control Plasmid DNA (SHC004); knockdown plasmids (hereby referred to as shRNA1 and shRNA2) were: CYBRD1 MISSION® shRNA Plasmid DNA cytochrome b reductase 1 (Human, SHCLND-NM_024843), shRNA1: TRCN0000236452, shRNA2: TRCN0000236455. Cells were transfected
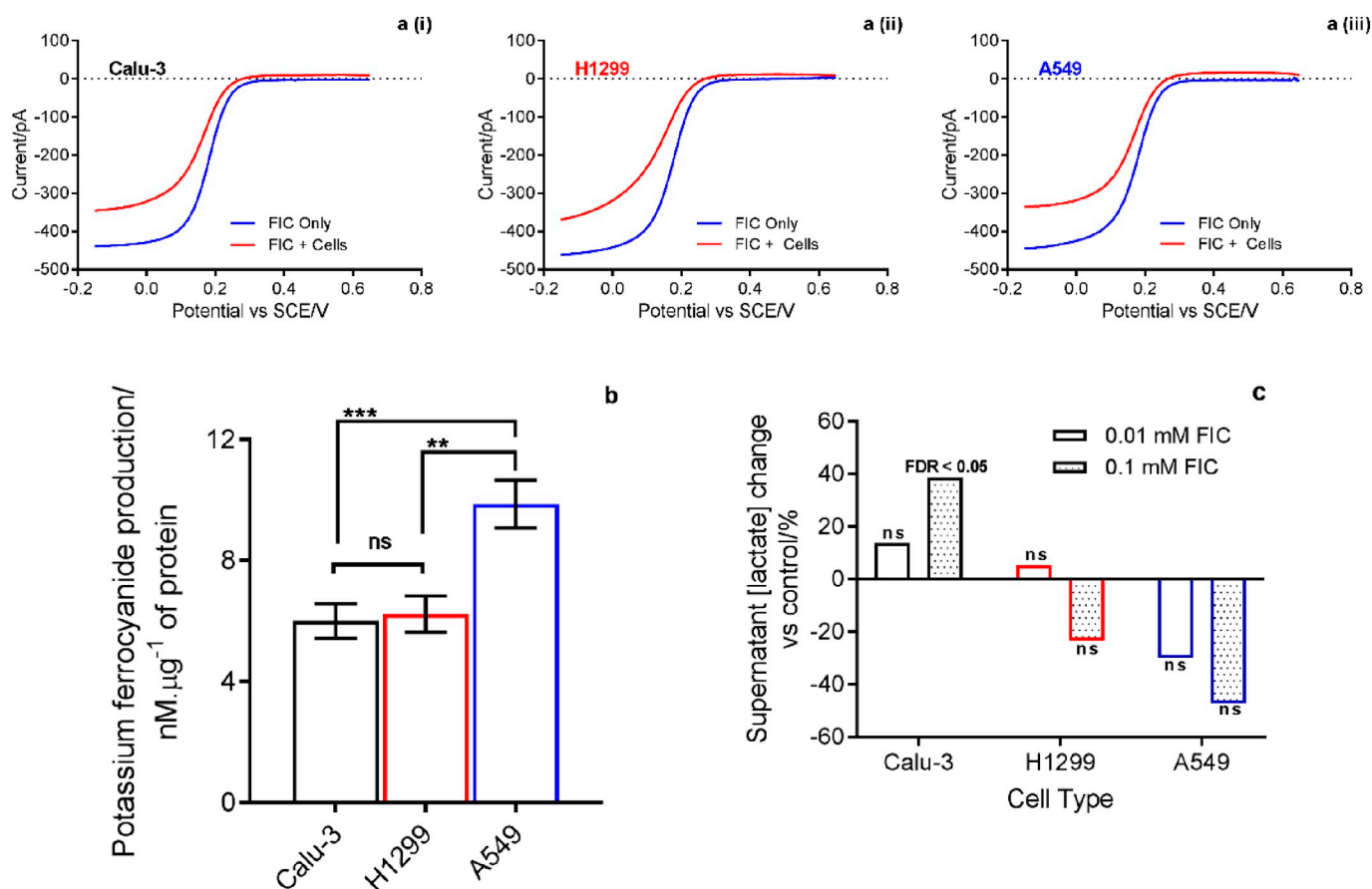
Fig. 1. Reduction of ferricyanide (FIC) upon incubation with of Calu-3, H1299 and A549 cells, and metabolomics analysis of spent medium showing lactate change. Cells with no increase of intracellular ascorbate levels used in the experiment.

(a) Typical linear sweep voltammograms of FIC (0.1 mM) reduction for (i) Calu-3, (ii) H1299, and (iii) A549 cells. Scanned from a 650 to $-150\,\text{mV}$, $10\,\text{mV.s}^{-1}$. (b) Potassium ferrocyanide (FOC) production, on incubation with 0.1 mM FIC, as a measure of FIC reduction by cells - without increased intracellular ascorbate; $N = 3$, $n = 3$. Calu-3 and H1299 cells values significantly lower compared to A549 cells at $P = 0.0009$ and $P = 0.0013$, respectively. (c) Metabolomics analysis of spent media of Calu-3, H1299 and A549 cells incubated with ferricyanide (FIC) in Hanks' Balanced Salt Solution (HBSS), relative to control cells in respective buffer only. Changes in lactate metabolite are shown. False discovery rate (FDR) of < 0.05 for Calu-3 cells indicates significant difference.

Statistical analysis performed between cell types in figures (a) and (b) were made using two-way ANOVA with Tukey's multiple comparison test; $p < 0.05$ considered statistically significant. For all comparisons: $*p < 0.05$, $**p < 0.01$, $***p < 0.001$. N = 3, n = 3. All values represent mean from three biological replicates $\pm$ SEM. Figure (c) data was analysed *via* t-test using Metaboanalyst, with significance between samples said to be present if the false discovery rate (FDR) was < 0.05. $N = 6$, $n = 1$.

following the manufacturer's protocol for Lipofectamine™ 3000 reagent (ThermoFisher Scientific Ltd). Cells were grown for one day for A549 and H1299 cells, or two days for Calu-3 cells, and were transfected with the appropriate plasmids using Lipofectamine 3000 and Gibco™ Opti-MEM™ Reduced Serum Media (ThermoFisher Scientific Ltd) as the transfection medium. The cells were then cultured for a further two days without removal of medium prior to any further experimental work. To determine transfection efficiency the cells were seeded in 24 well plates at 1.25×10^5 for Calu-3 cells, or 5×10^4 for H1299 and A549 cells, in 1 mL of DMEM, and transfected according to the protocol outlined above. A non-transfected control was also grown. Following completion of the growth period, cells were harvested using 250 µL accutase per well. Once detached 250 µL of DMEM was added to each well to stop the action of the accutase, and the cells were pelleted *via* centrifugation at $300\,g$ for 5 min. The resulting pellet was washed in phosphate buffered saline (PBS) and then samples were tested for transfection efficiency (green channel fluorescence) using a flow cytometer. All flow cytometry was carried out in collaboration with The University of Nottingham Flow Cytometry Facility, using a FC500 Series Flow Cytometer (Backman Coulter Ltd). All analysis was carried out using Kaluza, Analysis Version 1.5. Please note due to minimal transfection efficiency for the Calu-3 cells, only A549 and H1299 cells

were assayed further. This experiment was carried out with two technical repeats and three biological repeats.

2.14. RT-qPCR for CYBRD1 knockdown

H1299 and A549 cells were seeded in 6 well plates at $2.5 \times 10^5/$ well and grown for 24 h, and transfected according to the above section. The cells were washed with 1 mL PBS prior to harvesting by the addition of 0.5 mL accutase until detachment. 0.5 mL warm DMEM was added, and the cells pelleted by centrifugation at $300\,g$ for 5 min. The resulting pellet was washed using warm PBS and centrifugation, as described above. On ice, the pellet was lysed and RNA extraction was carried out in line with the manufacturer's protocol for RNeasy mini kit (Qiagen Ltd., Cat No./ID: 74104). Following RNA extraction, the purified RNA was tested for RNA content using a NanoDrop 1000 Spectrophotometer (ThermoFisher Scientific Ltd). cDNA was prepared *via* reverse transcription as outlined in the Quantiscript Reverse Transcriptase kit (Qiagen Ltd., Cat No./ID: 205311). Quantitative polymerase chain reaction (qPCR) was used to amplify the prepared cDNA using primers designed using Roche ProbeFinder, and then checked for veracity using USCS In-silico PCR software. Primers for CYBRD1 (accession no. NM_024843) crossed an exon-exon boundary,
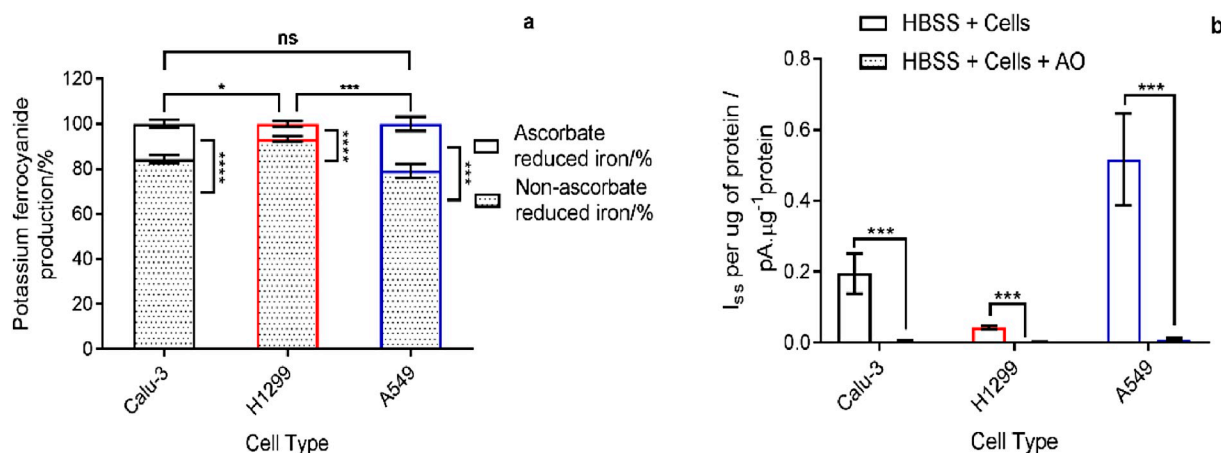
Fig. 2. Ascorbate's role in extracellular iron reduction; assessed in the presence of specific ascorbate oxidizing agent, ascorbate oxidase (AO).
(a) Potassium ferrocyanide 'production' attributed to extracellular ascorbate and non-extracellular ascorbate reduction of extracellular potassium ferricyanide (FIC), for comparison between of extracellular ascorbate-mediated tPMET of the cell lines. Ferricyanide reduction attributable to extracellular ascorbate was significantly different between both Calu-3 and A549 cells *vs* H1299 cells at $P = 0.0267$ and 0.0007, respectively (b) Ascorbate 'removal'; analysed voltammograms for presence and absence of AO. AO+ wells were set up in parallel to AO- wells and the ascorbate attributable currents in each measured to provide the values presented in figure b, a HBSS only (no cell incubation) current was subtracted as a baseline to obtain ascorbate release currents.
Statistical analysis performed using two-way ANOVA with Tukey's multiple comparison test; $p < 0.05$ considered statistically significant. All univariate comparisons were made using one unpaired *t*-test per data set (cell type) with Holm-Sidak determination of significance; $p < 0.05$ considered statistically significant. For all comparisons: *$p < 0.05$, **$p < 0.01$, ***$p < 0.001$. $N = 4$, $n = 3$. All values represent mean from three biological replicates $\pm$ SEM.

and were of the following sequences: For. 5′ - TTGGACTGATAGCTGT CATATGCT - 3′, Rev. 5′ - GAAATGCTCGGAGAGAAAGC- 3′. Glyceraldehyde-3-phosphate dehydrogenase (GAPDH) primer pair was provided by the David Heery laboratory (The Gene Regulation Group, The University of Nottingham). Primer sequences for the GAPDH housekeeping primer were: For. 5′ - AGGTGAAGGTCGGCGTCAA - 3′, Rev. 5′ - GATGACAAGCTTCCCGTT- 3′. Relative quantification of CYBRD1 gene expression by real-time PCR was performed according to the manufacturer's protocol for the Brilliant II SYBR® Green QPCR Master Mix (Agilent Technologies Ltd., #600828), using a Stratagene Mx3005P thermocycler (Stratagene Ltd). This experiment was carried out with twelve technical repeats and three biological repeats.

2.15. Flow cytometry for DCYTB knockdown

H1299 and A549 cells were seeded in 24 well plates at 5×10^4 and incubated for 24 h. The cells were transfected as described in the above section. Cells were detached using 250 μL accutase per well. Once detached, 250 μL of DMEM was added to each well to stop the action of the accutase, and the cells were pelleted *via* centrifugation at 300 *g* for 5 min. The resulting pellet was washed in PBS. The cells were then fixed using 4% paraformaldehyde for 15 min, prior to three subsequent washes with ice-cold PBS to remove any residual paraformaldehyde. The samples were blocked/permeabilised for 5 min using 1% PBA (PBS with 1% bovine serum albumin) and 0.1% tween-20. The cells were pelleting *via* centrifugation (300 *g*, 5 min), before primary staining for 30 min at 8 μg/mL in 1% PBA (ab66048, anti-cytochrome *b* reductase 1, Abcam Ltd). A secondary only control sample was also set up for each plasmid transfection, which was incubated with only 1% PBA/0.1% tween-20 (no antibody). Following staining, 1 mL 1% PBA was added, and the samples were centrifuged at 300*g* for 5 min. The samples were then secondary stained for 15 min at 2 μg/mL, for all wells (Donkey anti-Rabbit IgG (H + L) Highly Cross-Adsorbed, Alexa Fluor® 647, A31573, ThermoFisher Scientific Ltd). Following completion of staining, 1 mL 1% PBA/0.1% tween-20 was again added and the cells pelleted. The samples were resuspended in 500 μL 1% PBA/0.1% tween-20 prior to transportation to the flow cytometer on ice (FC500 Series Flow Cytometer, Beckman Coulter Ltd). 25 μL 50 μg/mL propidium iodide was added to one positive control sample, to ensure fixation and

permeabilisation had been effective. Laser lines for selected fluorophores were as follows: AlexaFluor® 647: Beckman Coulter FC500, 633 laser line, emission 655–685 nm; green fluorescent protein (GFP): Beckman Coulter FC500, 488 laser line, emission 514–542 nm; propidium iodide: Beckman Coulter FC500, 488 laser line, emission 612–638 nm. Please note that examples of gating for flow cytometry are displayed in Fig. S6c. This experiment was carried out with one technical repeats and four biological repeats.

2.16. Electrochemical analysis of transfected cells

H1299 and A549 cells were seeded in 6 well plates at $2.5 \times 10^5/$ well, and transfected according to the above section. Following growth period, each plasmid transfection ($2\times$ control plasmid, $2\times$ shRNA1 plasmid and $2\times$ shRNA2 plasmid) were incubated with HBSS only or 0.01 mM potassium ferricyanide (FIC) in HBSS, for 2 h. The supernatants were tested electrochemically, as outlined in the 'electrochemical analysis' section. This assay was repeated using the control plasmid only, alongside non-transfected samples, to allow for accurate comparison between non-transfected and transfected cell tPMET. This experiment was carried out with one technical repeats and four biological repeats.

2.17. Mitochondrial membrane potential upon transfection

H1299 and A549 cells were seeded in 96 well plates at $8.4 \times 10^4/$ well in 150 μl DMEM, and transfected according the above protocol. Upon completion of growth, the cells were incubated for 2 h with either DMEM, negative control, 25 μM Carbonyl cyanide-4-phenylhydrazone (FCCP, positive control), or HBSS. Each reagent was triplicated. This was to simulate the two-hour HBSS/FIC incubation carried out for electrochemical analysis. Mitochondrial membrane potential was assessed using the JC-1 (5,5′,6,6′-Tetrachloro-1,1′,3,3′-tetraethylbenzimidazolylcarbocyanine, iodide) dye (Biotium, Inc.). Preparation of the JC-1 reagent stock was as follows: 1 mg/mL was prepared dissolving 5 mg JC-1 powder in 5 mL DMSO, prior to vortexing to ensure homogeneity. The vial was left at room temperature for ~ 15 min to ensure complete dissolution. Dissolved JC-1 stock was then aliquoted out into 200 Eppendorfs of 25 μL each (provided at this
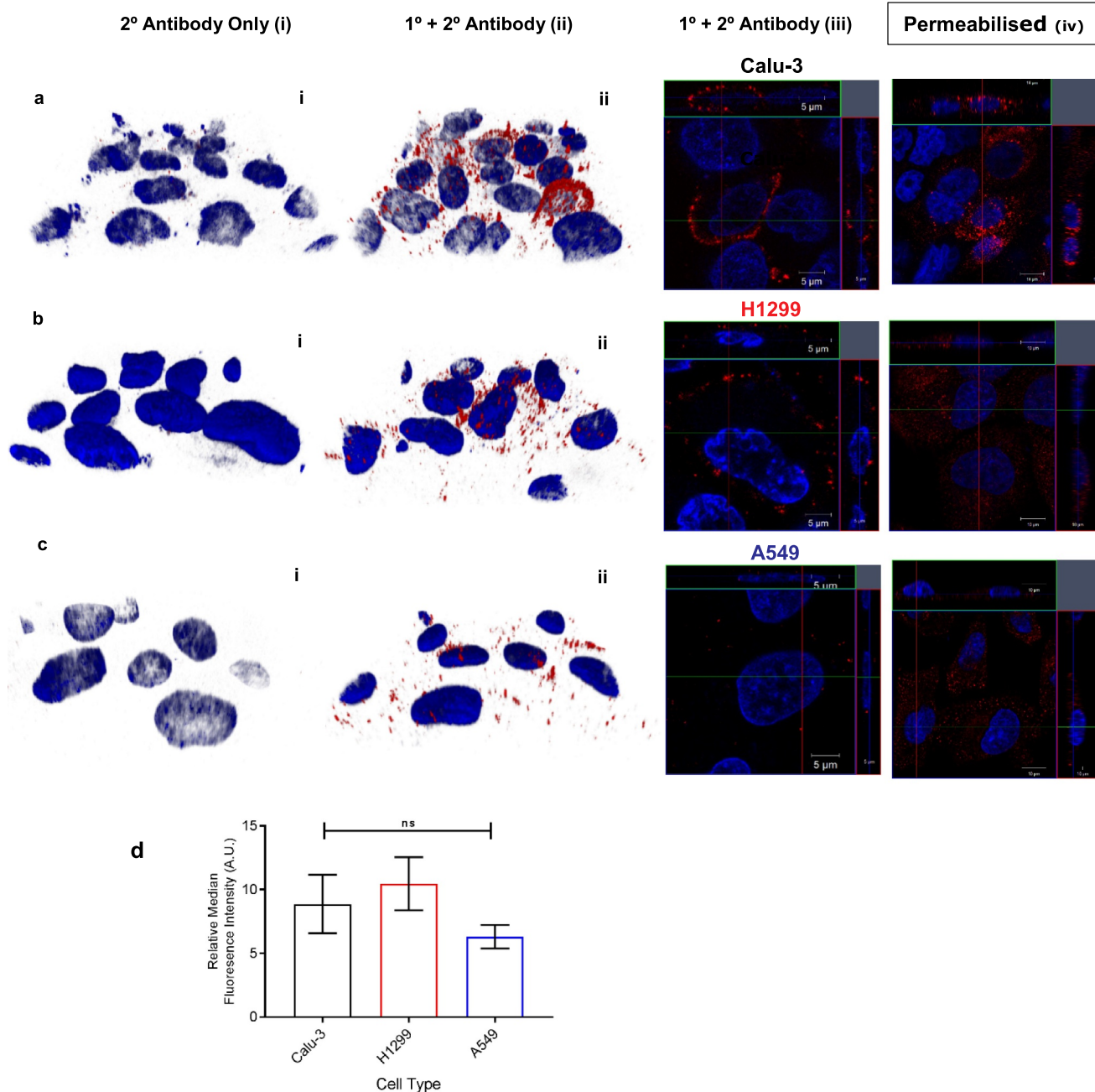
Fig. 3. Duodenal cytochrome *b* (Dcytb) immunostaining of (a) Calu-3, (b) H1299 and (c) A549 cells.
Focus stack images are shown as 3D rendered images (i and ii) or in orthogonal views (iii) and permeabilised cells iv). Antibody combinations were as followed: (i) Secondary antibody only, 2 µg/mL Alexa 647. (ii) Primary antibody (ab66048) 10 µg/mL, and secondary antibody, 2 µg/mL Alexa 647. (d) Flow cytometry for Dcytb in non-transfected Calu-3, H1299 and A549 cells.

preparation). For the JC-1 assay, a $1\times$ staining solution was prepared by diluting 25 µL of $200\times$ JC-1 stock in 5 mL DMEM. This preparation was then vortexed and incubated at room temperature for 1–2 min. 50 µL of $1\times$ JC-1 staining solution was added to each well, and incubated for 15 min. Following this incubation, the reagent was removed and the cells were washed with 50 µL PBS per well. The fluorescence was then measured using a Tecan Microplate Reader (Tecan Ltd., Weymouth, UK). Fluorescence of JC-1 aggregates (red) was measured at $\lambda_{ex.}$ 550 nm/$\lambda_{em.}$ 600 nm, and green fluorescence of JC-1 monomers measured at $\lambda_{ex.}$ 485 nm/$\lambda_{em.}$ 535 nm. The ratio of red/green fluorescence was determined, with a higher ratio indicating more intact mitochondrial membrane activity. This experiment was carried out with three technical repeats and four biological repeats.

2.18. Cellular redox activity and membrane perturbation upon transfection

H1299 and A549 cells were seeded and transfected in 96 well plates according to the above protocols. The cells were incubated for two hours with HBSS to simulate electrochemical assay conditions. The MTS assay and lactate dehydrogenase (LDH) assays were then performed on the same samples to determine cellular metabolic activity and membrane perturbation, respectively. The protocols for these assays, following reagent incubation, are as outlined previously [61]. These experiments were carried out with three technical repeats and four biological repeats.
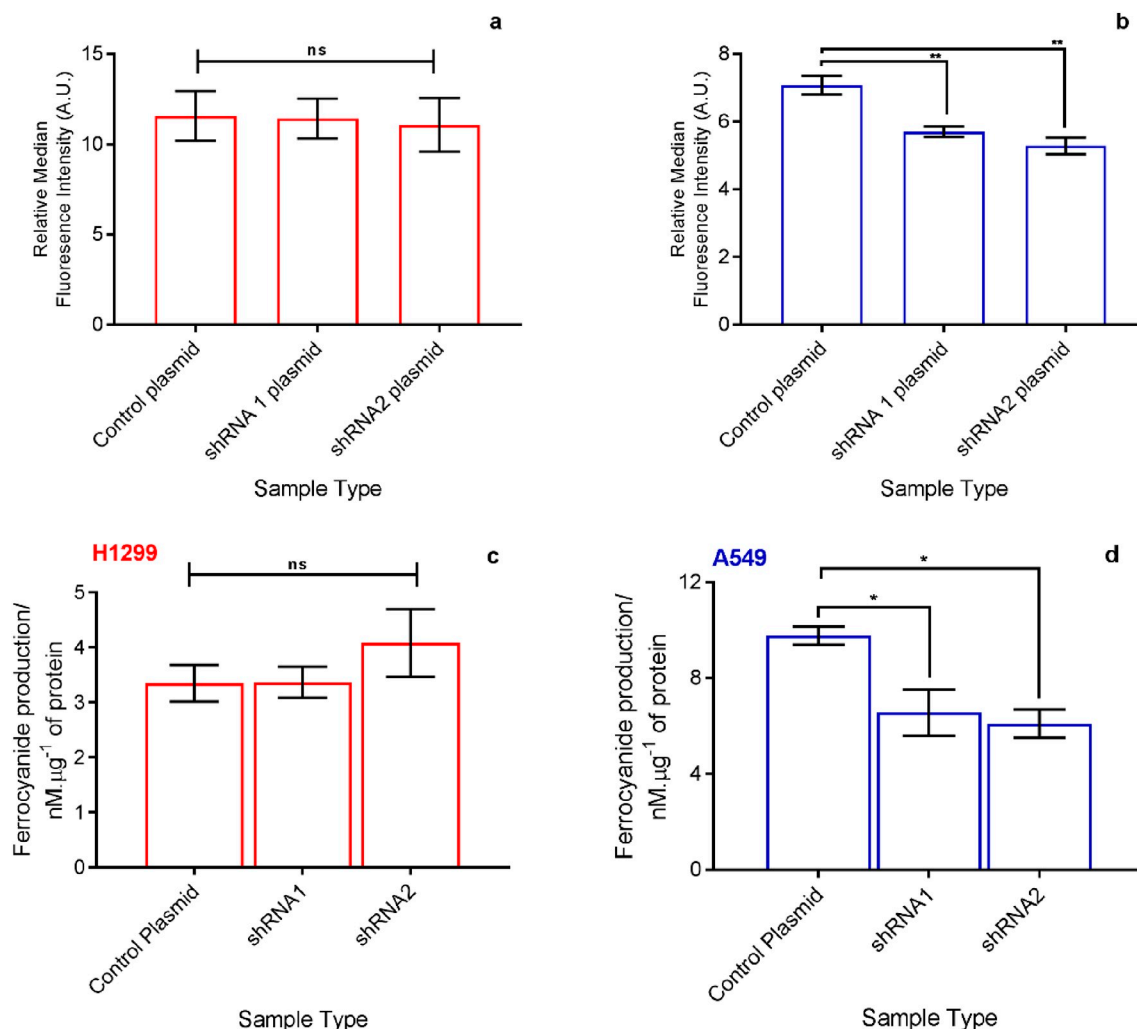
Fig. 4. Duodenal cytochrome *b* (Dcytb) involvement in trans plasma membrane electron transport.
(a and b) Flow cytometry for Dcytb protein when cells were transfected with control and knockdown plasmids; (a) H1299, (b) A549 (representative histograms obtained which were used to construct these bar charts can be seen in Fig. S7). $N = 4$, $n = 1$. A549 cells showed a significant reduction in Dcytb protein expression at $P = 0.006$ and 0.001 for shRNA 1 and shRNA 2 *vs* control, respectively. H1299 cells showed no significant change. (c and d) Electrochemical analysis of the reduction of 0.01 mM potassium ferricyanide (FIC) by cells transfected with control or knockdown plasmids; $N = 4$, $n = 1$; (c) H1299, (d) A549. A549 cells showed a significant reduction in tPMET activity (*i.e.* FOC production) at $P = 0.028$ and 0.013, shRNA1 and shRNA2 *vs* control, respectively. H1299 cells showed no significant change. Statistical analysis performed using one-way ANOVA with Tukey's multiple comparison test; $p < 0.05$ considered statistically significant. For all comparisons: *$p < 0.05$, **$p < 0.01$, ***$p < 0.001$. All values represent mean from three biological replicates ± SEM.

2.19. Statistical analysis

All statistical analysis was performed using GraphPad Prism 7.01, whereby $p < 0.05$ was considered statistically significant. Appropriate statistical tests were chosen depending on the requirement for one and two factor analysis of variance, with appropriate *ad hoc* hypothesis tests.

3. Results

3.1. Linear sweep voltammetry as a method to study tPMET

We recently developed and applied a new electrochemical based assay, using linear sweep voltammetry, to identify different external electron flux rates. This assay was applied to A549, Calu-3 and H129 cells, and these cell types were also used in the current study [61]. The assay quantitates the electrical charge which is transferred across the plasma membrane *via* an iron redox reporter molecule, as described in the supporting information (Fig. S1). The important component of the graphs Fig. 1a which represents the magnitude of the external charge

flux by the cells is the steady state current observed at approximately 0.3 V. The value of this is proportional to the number of FIC molecules reduced by the cell to FOC. The FOC is then electrochemically oxidised yielding a steady state anodic current which is measured and plotted in Fig. 1 b. Fig. 1 therefore shows reduction capacity of tested cells, indicating similar levels for Calu-3 and H1299 cells and significantly higher level for A549.

The data further show that the presence of higher concentration of FIC - the redox state of iron known to affect cellular metabolism - has an effect on lactate metabolism of Calu-3, whilst for H1299 and A549 cells there was no detectable change in the metabolism of lactate upon FIC incubation (Fig. 1c). Lactate was selected as marker because its metabolism is implicated in regenerating NAD^+ levels in cancer [68]. This draws a parallel to the use of NADH by tPMETSs for the regeneration of NAD^+. This is noteworthy as it may suggests that the upregulation of lactate metabolism may work in tandem with higher tPMET activity in Calu-3 cells, implying a link between energy reprogramming and tPMETs which is an essential trait of cancer.

Here we first apply linear sweep voltammetry to investigate tPMET activity in selected cell lines. We hypothesised that two routes of trans-
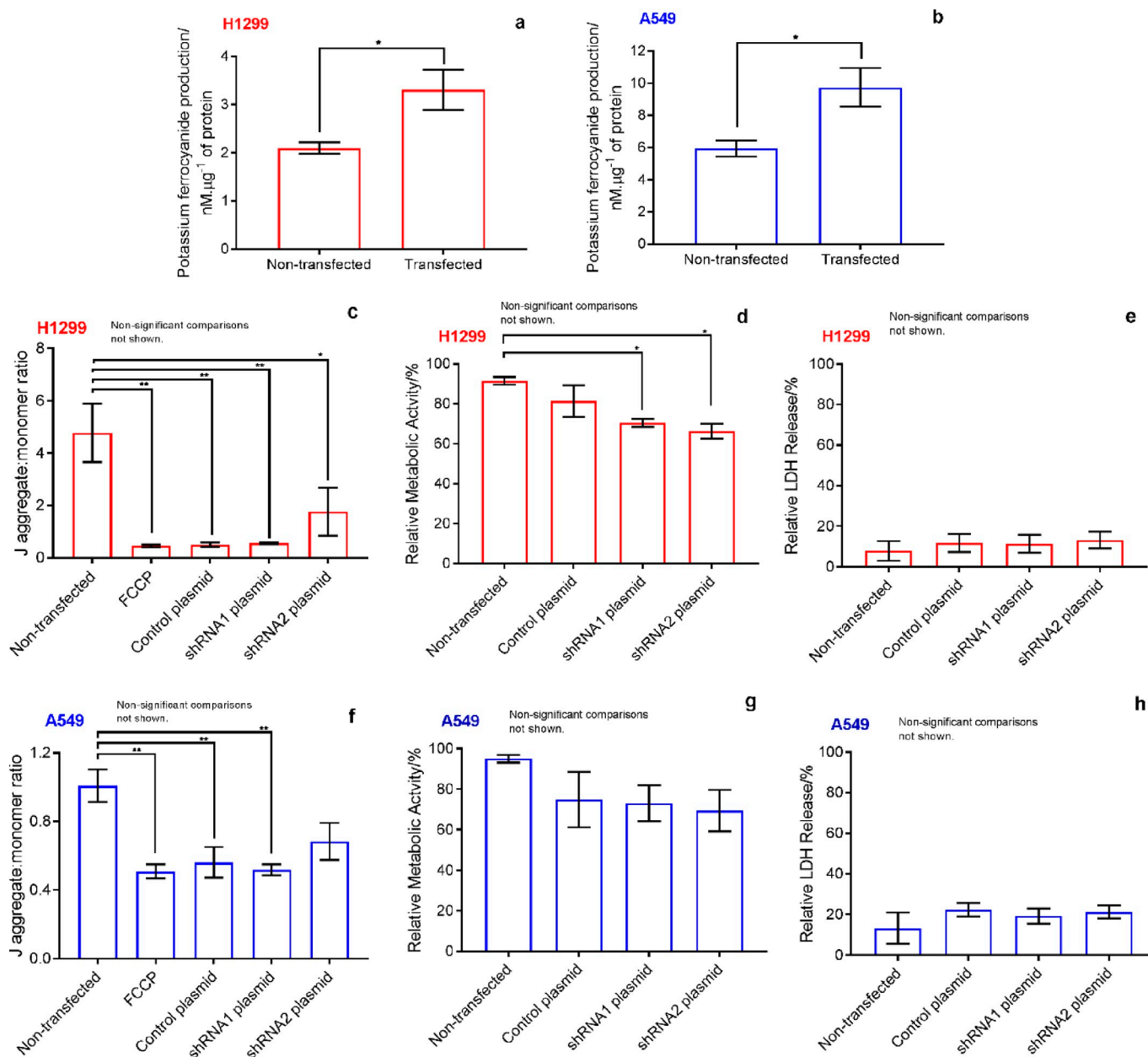
Fig. 5. (a-h) Trans plasma membrane electron transport is upregulated in response to mitochondrial stress.
(a and b) Electrochemical analysis of cellular reduction of 0.01 mM potassium ferricyanide into ferrocyanide in cells transfected with control plasmid and non-transfected counterparts; $N = 4$, $n = 1$. Increases in tPMET activity following transfection were observed for both H1299 and A549 cells (H1299, $P = 0.0229$; A549, $P = 0.0304$). (c and f) JC-1 assay for mitochondrial membrane potential; $N = 4$, $n = 3$. No significant difference was found between FCCP incubated cells and transfected cells, with significant differences compared to a non-transfected control of $P = 0.002$, 0.003 and 0.034 or H1299 (Fig. 5c) control, shRNA1 and shRNA2 plasmids, respectively. For A549 cells (Fig. 5f) a similar trend was observed with control and shRNA1 plasmids showing a significant decline compared to non-transfected cells of $P = 0.009$ and 0.004, respectively; (d and g) MTS assay for cellular metabolic activity; $N = 4$, $n = 3$; No significant reductions in MTS activity were observed compared to a non-transfected control besides for the knockdown plasmids of H1299 cells (shRNA1, $P = 0.033$; shRNA2, $P = 0.011$). (e and h) Lactate dehydrogenase (LDH) assay; $N = 4$, $n = 3$; No significant changes for all samples were observed (f-h) Statistical analysis performed using one-way ANOVA with Tukey's multiple comparison test; $p < 0.05$ considered statistically significant. Univariate comparisons (a and b) were made using unpaired t-test $p < 0.05$ considered statistically significant. For all comparisons: *$p < 0.05$, **$p < 0.01$, ***$p < 0.001$. All values represent mean from three biological replicates ± SEM.

plasma membrane electron transport in cancer cells could occur; one *via* direct electron transfer using DcytB, and second occurring by a mediated process involving ascorbate.

3.2. Ascorbate efflux as a trans plasma membrane electron transport system (tPMETS)

To confirm that ascorbate plays a role in shuttling electrons leading to FIC reduction into FOC (Fig. 1), cells were incubated with the ascorbate-specific oxidising agent, ascorbate oxidase (AO) in the and presence of FIC (Fig. 2a) and its absence (Fig. 2b). The AO removed ascorbate from the medium. Electrochemical analysis and assessment of the magnitude of the anodic current at approximately 0.3 V was performed in the presence and absence of AO with FIC (Fig. 2a). Consequently, any differences observed in oxidative currents associated with FOC oxidation could be attributed to the reduction of FIC to FOC by ascorbic acid. This therefore allows for tPMET activity to be calculated and attributable to extracellular ascorbate. To conduct the study, a
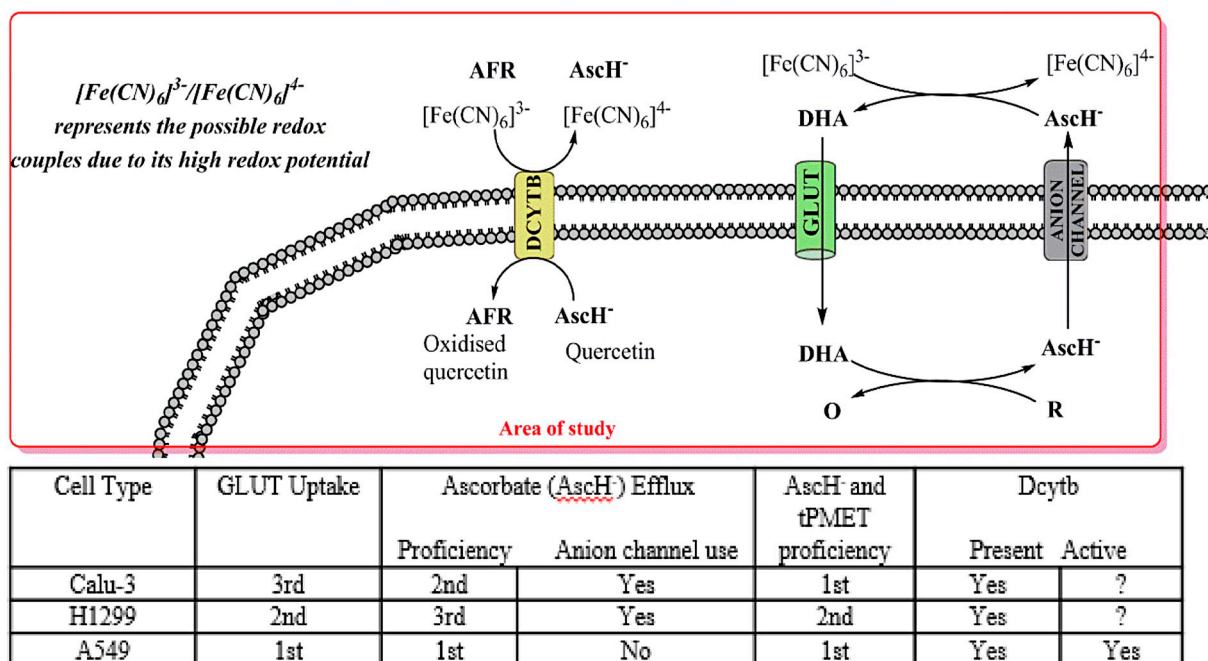
Fig. 6. Summary of findings. tPMET may occur using Dcytb or ascorbate shuttling, and this varies between the cells. tPMET enzymes/transporters: DCYTB (duodenal cytochrome b_{561}), GLUT (glucose transporter). Redox co-factors: AscH (ascorbate monoanion), AFR (ascorbate free radical), DHA (dehydroascorbate), $[Fe(CN)_6]^{3-}$/$[Fe(CN)_6]^{3-}$ (ferricyanide/ferrocyanide (reduced/oxidised), O, oxidised redox co-factor, R, reduced redox co-factor (where R/O can include NADH/NAD$^+$ (nicotinamide adenine dinucleotide (reduced/oxidised)), NADPH/NADP$^+$ (nicotinamide adenine dinucleotide phosphate (reduced/oxidised)), GSH/GSSG (glutathione/glutathione disulphide (reduced/oxidised)).

signal (current) amplification associated with FIC reductions (voltammogram Fig. S1) was achieved by loading of the cells with DHA which was transported into the cell using GLUT transporters (Fig. S2) and converted to ascorbic acid (Fig. S3). The data in Fig. 2 illustrate that all cell lines tested employ effluxed extracellular ascorbate to reduce extracellular FIC, but differ in their proficiency to do this.

Regarding Calu-3 and A549 cells, the FIC reduction attributable to extracellular ascorbate was no different between the cell lines, with values of 15.6% and 20.9%, respectively (Fig. 2a). The FIC reduction attributable to extracellular ascorbate was significantly different between Calu-3 and A549 cells *versus* H1299 cells, with the significantly lower portion of extracellular ascorbate-mediated tPMET at 6.7% for H1299 cells (Fig. 2a). Fig. 2b shows data obtained for cells treated with ascorbate oxidase in the absence of FIC. This confirms that the difference observed in Fig. 2a is attributable to ascorbate efflux. It should be noted that the data in Fig. S4 and S5 confirm that the efflux of ascorbate in all three cell types tested occurs *via* anion channels, inhibited by glucose transport inhibitors (DIDS and SITS), whereby in Calu-3 cells the data also point to the involvement of volume-sensitive anion channels (VSAC).

An interesting observation is that the tPMET activity increases significantly upon ascorbate supplementation. When 'loaded' with ascorbate *via* DHA incubation, the tPMET activity, as measured by FIC production, was 129, 141 and 171 nM FOC *per* μg of protein for Calu-3, H1299 and A549 cells, respectively. Compared to the basal tPMET level (Fig. 1) this represents a 21.5, 22.7 and 17.4 fold change in FOC produced *per* μg of protein for Calu-3, H1299 and A549 cells upon increasing intracellular ascorbate.

3.3. Duodenal cytochrome b (Dcytb) role as a direct electron tPMET

The images and flow cytometry data in Fig. 3 show live-cell immunostaining, which demonstrates the presence of Dcytb in the cancer cell lines tested. The images depict Dcytb protein staining (in red) forming a 'halo' at a distance from the cell nuclei (in blue) in non-

permeabilised cells. The orthogonal images in Fig. 3iii, relative to Fig. 3 iv confirm this location of the staining. As the immunostaining procedure was conducted on ice, with no permeabilisation or fixation of the cells, the experiment would hence indicate the presence of Dcytb at the plasma membrane of the cells. The location of Dcytb is important in the context of its role in tPMET as, by definition, tPMET must occur through the transfer of electron across the plasma membrane.

3.4. Dcytb acts as tPMET syste in A549 cells

To determine the role of Dcytb in tPMET, we transfected cells with shRNA-expressing plasmids (shRNA1 and shRNA2) to knockdown the Dcytb-encoding gene *CYBRD1*. Transfection data show (Fig. S6a) significant differences in efficacy, with very low levels obtained for Calu-3 cells with both plasmids. In H1299 cells a significant knockdown of *CYBRD1* was achieved with the shRNA1 plasmid, and in A549 cells with both shRNA1 and shRNA2 plasmids (Fig. S6b). At the protein level, data show no significant knockdown of Dcytb protein expression for H1299 cells, but a significant difference for both knockdown plasmids in A549 cells, compared to the control (Fig. 4a and b).

Electrochemical assays made comparisons between transfected H1299 and A549 cell lines, as the cells with the least and the most proficient ascorbate shuttling mechanisms (as *per* Fig. 2a). No statistically significant reduction in tPMET activity was observed for H1299 cells upon Dcytb knockdown, relative to control plasmid transfected cells (Fig. 4c and d), which would be expected as per absence of knockdown effect at the protein level (Fig. 4a and b). A significant reduction in FOC production in A549 cells (Fig. 4d) suggests a prominent role for Dcytb in tPMET activity. Since no change in Dcytb protein level was observed for H1299 cells, we cannot conclude that Dcytb acts as a tPMET in this cell line. However, the presence of Dcytb confirmed by immunostaining suggests this is likely possible.

3.5. Trans plasma membrane electron transport is upregulated in response to mitochondrial stress

We should point out to an interesting side observation seen for cells transfected with the control plasmid. Data in Fig. 4 show an upregulation of tPMET activity in H1299 (Fig. 4c, control plasmid) and A549 (Fig. 4d, control plasmid) transfected cells, compared to the basal levels in the range of 2 and 5 nM/μg protein seen using the same FIC concentration, respectively observed under same experimental conditions in our previous published study using 0.01 mM of FIC [61]. A comparison to Fig. 1 was not made as a higher FIC concentration was used which can alter the tPMET activity. A lower concentration of 0.01 mM was used to maximise our signal to noise ratio. To investigate this further, biochemical assays were conducted to elucidate if a link between cellular stress, due to transfection process, and tPMET activity may exist in H1299 and A549 cells (Fig. 5).

Fig. 5a and b compare FOC production in non-transfected, control cells and cells transfected with the control plasmid. The data clearly indicate a significant difference in FOC production, i.e. oxido-reductive capacity of the cells, with a clear increase for the transfected counterparts. The analysis of mitochondrial membrane potential, shows a significant reduction in transfected A549 and H1299 cells, comparable in extent to carbonyl cyanide-*p*-trifluoromethoxyphenylhydrazone (FCCP), a compound which causes depolarisation of the mitochondrial membrane (Fig. 5c and f). MTS assay data on cellular metabolic activity of transfected cells showed some reduction (Fig. 5d and g), where it should be noticed that MTS assay reflects activity of NAD(P)H-dependent oxidoreductase enzymes which are present mainly in the cell cytosol [69] and the data would hence indicate that despite a dramatic decrease in mitochondrial membrane potential, cellular metabolic activity was largely maintained. Lactate dehydrogenase (LDH) assays showed no significant difference compared to the non-transfected control, indicating no necrotic process occurring (Fig. 5e and h). We would thus tentatively suggest that the results indicate that the activity of tPMET is upregulated when the cell experiences mitochondrial stress, and that this may play role in maintaining cellular redox capability [7,17].

4. Discussion

In this study we have investigated two mechanisms by which electrons are transported across the cell cytoplasmic membrane from three lung cancer cell models. The aim of the study was to establish what tPMET systems cells use to inform on their role in bioenergetics. One mechanism was found to occur *via* an ascorbate-mediated tPMET system and contributes differently to the overall oxido-reductive capacity of the cells with 20.9% for A549, 6.7% for H12199, and 15.5% for Calu-3 cells. The data confirmed that ascorbate is transported *via* an anion transporter across the plasma membrane in all three cell lines, whereby Calu-3 cells may also employ a volume-sensitive anion channel (Figure S4). Once transported outside of the cells, ascorbate then passes an electron on to FIC present in the medium (Fig. 6), as proven by cell treatment with ascorbate oxidase; the enzyme reduced the ascorbate mediated electrochemical signal to effectively zero. Our results however contrast the data in non-malignant bronchial epithelial cells, whereby ascorbate supplementation did not increase iron uptake [9], although it should be noted that the study did not measure tPMET activity directly as in our study, rather cellular iron conctrations. Moreover, it has been suggested that the reducing equivalent for Dcytb intracellularly is ascorbate [70], although quercetin has also been proposed as an electron sink [71].

The second mechanism we identified contributing to transmembrane electron transport is the ferrireductase duodenal cytochrome *b* (Dcytb). All tested cell lines express Dcytb protein, as confirmed by immunostaining. Successful knockdown of Dcytb gene in A549 cells conforms its role as a tPMET in this cell type, however we could not establish its role in other tested cells as *per* unsuccessful knockdown.

Overall, the way the cells use these tPMET systems differs between them, as evidently seen for ascorbate transport. The key importance of our work is to realise the heterogeneity in the use of these systems by different cell types and its importance for drug discovery of molecules that target these systems for *e.g.* cancer therapy [71,72]. For instance, if one were to target ascorbate-shuttle based tPMET in H1299 cells it would be a less successful approach compared to A549 and Calu-3 cell types.

The latter part of our study has drawn a link between depolarisation of mitochondrial membrane potential in transfected cells and an increase in plasma membrane charge transfer. Other studies also observed similar higher tPMET levels when mitochondria are dysfunctional [7,17,23,73].

The current studies in the field are focusing on deciphering how more than one energy metabolism mechanism may exist in malignant tumour cells – the Warburg effect [18,19,43,44,75–77] and the reverse Warburg effect may be occurring [78–80]. The reverse Warburg effect has been described, in which cancer cells use reactive oxygen species (ROS) to induce the Warburg effect in cancer-associated fibroblasts (CAF), and then utilise the cell-exported lactate and pyruvate metabolites to increase the rate of oxidative phosphorylation. There is evidence *in vivo* that in some lung tumours a switch from oxidative to glycolytic metabolism does not occur, the latter would be predicted by the Warburg effect [81]. It is also noted that there is a high degree of metabolic heterogeneity between different tumours (all non-small cell lung cancers with varying histology) and between similar tumour types, so the hypothesis that tPMET may be targeted to induce anti-proliferative effects in malignant cells is still valid. There is also mounting evidence that targeting mitochondrial metabolism in cancer may be viable route of therapy [82], and its use in tandem with the targeting of tPMET may prove useful in future drug discovery. Our data suggest that to target therapy against tPMET systems it is of paramount importance to understand tPMET heterogeneity in difference cell types and cancers.

Contributions

These authors contributed equally to this work: H.G.S., F.J.R and S.S.

F.J.R and S.S. supervised this project and had intellectual input into all experiments. H.G.S., F.J.R., S.S., H.C., J.E. conceptualised gene knockdown work, with H.G.S designing, performing and analysing the data. H.C. also aided in the design of *CYBRD1*-targeting primers. R.M. and H.G.S. designed, performed and analysed immunocytochemistry experimental work. A.A. and H.G.S. designed, performed and analysed metabolomics work, with intellectual input from D.H.K. in conceptualisation and analysis of these experiments. H.G.S designed and performed mitochondrial membrane potential (JC-1) assay, with R.C. aiding in the design and interpretation of the data. All other experimental work was performed and analysed by H.G.S. The manuscript was prepared by H.G.S., F.J.R and S.S., with additional contributions and edits from all authors.

Transparency document

work, the Zeiss Elyra PS1 microscope facility.

Funding

Appendix A. Supplementary data

Supplementary data to this article can be found online at https://doi.org/10.1016/j.bbabio.2019.06.012.

References

[1] J.D. Ly, A. Lawen, Redox Rep. 8 (2003) 3–21.
[2] D. Del Principe, L. Avigliano, I. Savini, M.V. Catani, Antioxid. Redox Signal. 14 (2011) 2289–2318.
[3] J.M. Villalba, P. Navas, Antioxid. Redox Signal. 2 (2000) 213–230.
[4] A. del Castillo-Olivares, I.N. de Castro, M.A. Medina, Crit. Rev. Biochem. Mol. Biol. 35 (2000) 197–220.
[5] N. Grandvaux, M. Mariani, K. Fink, Clin. Sci. 128 (2015) 337–347.
[6] D. Sarr, E. Tóth, A. Gingerich, B. Rada, J. Microbiol. 56 (2018) 373–386.
[7] J.A. Larm, F. Vaillant, A.W. Linnane, A. Lawen, J. Biol. Chem. 269 (1994) 30097–30100.
[8] A.J. Ghio, J.L. Turi, F. Yang, L.M. Garrick, M.D. Garrick, Biol. Res. 39 (2006) 67–77.
[9] J.L. Turi, X. Wang, A.T. McKie, E. Nozik-Grayck, L.B. Mamo, K. Crissman, C.A. Piantadosi, A.J. Ghio, Am. J. Physiol. Lung Cell. Mol. Physiol. 291 (2006) L272–L280.
[10] A.T. McKie, D. Barrow, G.O. Latunde-Dada, A. Rolfs, G. Sager, E. Mudaly, M. Mudaly, C. Richardson, D. Barlow, A. Bomford, et al., Science 291 (2001) 1755–1759.
[11] M.A. Baker, G. Reeves, L. Hetherington, J. Müller, I. Baur, R.J. Aitken, Proteomics Clin. Appl. 1 (2007) 524–532.
[12] J. Rivlin, J. Mendel, S. Rubinstein, N. Etkovitz, H. Breitbart, Biol. Reprod. 70 (2004) 518–522.
[13] J.L. Wong, R. Créton, G.M. Wessel, Dev. Cell 7 (2004) 801–814.
[14] D. Del Principe, L. Avigliano, I. Savini, M.V. Catani, Antioxid. Redox Signal. 14 (2011) 2289–2318.
[15] D. Salvemini, W. Radziszewski, V. Mollace, A. Moore, D. Willoughby, J. Vane, Eur. J. Pharmacol. 199 (1991) 15–18.
[16] I. Savini, R. Arnone, A. Rossi, M.V. Catani, D. Del Principe, L. Avigliano, Mol. Membr. Biol. 27 (2010) 160–169.
[17] P.M. Herst, A.S. Tan, D.-J.G. Scarlett, M.V. Berridge, Biochim. Biophys. Acta 1656 (2004) 79–87.
[18] P.M. Herst, M.V. Berridge, Biochim. Biophys. Acta Bioenerg. 1767 (2007) 170–177.
[19] C. Grasso, L. Larsen, M. McConnell, R.A.J. Smith, M.V. Berridge, J. Med. Chem. 56 (2013) 3168–3176.
[20] O. Warburg (Ed.), J. Am. Med. Assoc. 96 (1931) 1982–2309.
[21] D. Hanahan, R.A. Weinberg, Cell 144 (2011) 646–674.
[22] D. Hanahan, R.A. Weinberg, Cell 100 (2000) 57–70.
[23] D.J. Scarlett, P. Herst, A. Tan, C. Prata, M. Berridge, Biofactors 20 (2004) 199–206.
[24] M.V. Berridge, A.N.S. Tan, Antioxid. Redox Signal. 2 (2000) 231–242.
[25] K.C. Patra, N. Hay, Trends Biochem. Sci. 39 (2014) 347–354.
[26] C.L. Linster, E. Van Schaftingen, FEBS J. 274 (2007) 1–22.
[27] X. Wang, A.J. Ghio, F. Yang, K.G. Dolan, M.D. Garrick, C.A. Piantadosi, Am. J. Physiol. Lung Cell. Mol. Physiol. 282 (2002) L987–L995.
[28] M.D. Garrick, K.G. Dolan, C. Horbinski, A.J. Ghio, D. Higgins, M. Porubcin, E.G. Moore, L.N. Hainsworth, J.N. Umbreit, M.E. Conrad, et al., BioMetals 16 (2003) 41–54.
[29] D.J.R. Lane, A. Lawen, J. Biol. Chem. 283 (2008) 12701–12708.
[30] A. Eccardt, T. Bell, L. Mattathil, R. Prasad, S. Kelly, J. Fisher, Antioxidants 6 (2017) 89.
[31] D.J.R. Lane, S.R. Robinson, H. Czerwinska, G.M. Bishop, A. Lawen, Biochem. J. 432 (2010) 123–132.
[32] J. M. May, Z. chao Qu, S. Mendiratta, Biochem. Pharmacol. 1999, 57, 1275–1282.
[33] O. Han, M.L. Failla, A.D. Hill, E.R. Morris, A.C. Smith, J. Nutr. 125 (1995) 1291–1299.
[34] J.X. Wilson, S. Jeffrey Dixon, Neurochem. Res. 14 (1989) 1169–1175.
[35] J.X. Wilson, C.E. Peters, S.M. Sitar, P. Daoust, A.W. Gelb, Brain Res. 858 (2000) 61–66.
[36] K. a Davis, S.E. Samson, K. Best, K.K. Mallhi, M. Szewczyk, J.X. Wilson, C.-Y. Kwan, A.K. Grover, Br. J. Pharmacol. 147 (2006) 131–139.
[37] J.M. May, Z.C. Qu, Mol. Cell. Biochem. 325 (2009) 79–88.
[38] J. M. Upston, A. Karjalainen, F. L. Bygrave, R. Stocker, 1999, 56, 49–56.
[39] J.M. May, L. Li, K. Hayslett, Z.C. Qu, Neurochem. Res. 31 (2006) 785–794.
[40] L. Skoza, A. Snyder, Y. Kikkawa, Lung 161 (1983) 99–109.
[41] I.D. Arad, H.J. Forman, A.B. Fisher, J. Lab. Clin. Med. 96 (1980) 673–681.
[42] R. Slade, K. Crissman, J. Norwood, G. Hatch, Exp. Lung Res. 19 (1993) 469–484.
[43] C. Prata, C. Grasso, S. Loizzo, F.V.D. Sega, C. Caliceti, L. Zambonin, D. Fiorentini, G. Hakim, M.V. Berridge, L. Landi, Leuk. Res. 34 (2010) 1630–1635.
[44] L. Côrte-Real, F. Mendes, J. Coimbra, T.S. Morais, A.I. Tomaz, A. Valente, M.H. Garcia, I. Santos, M. Bicho, F. Marques, J. Biol. Inorg. Chem. 19 (2014) 853–867.
[45] J. Du, J.J. Cullen, G.R. Buettner, Biochim. Biophys. Acta Rev. Cancer 1826 (2012) 443–457.
[46] E.J. Campbell, M.C.M. Vissers, C. Wohlrab, K.O. Hicks, R.M. Strother, S.M. Bozonet, B.A. Robinson, G.U. Dachs, Free Radic. Biol. Med. 99 (2016) 451–462.
[47] E.J. Campbell, M.C.M. Vissers, S. Bozonet, A. Dyer, B.A. Robinson, G.U. Dachs, Cancer Med. 4 (2015) 303–314.
[48] S.B. Vuyyuri, J. Rinkinen, E. Worden, H. Shim, S. Lee, K.R. Davis, PLoS One 8 (2013), https://doi.org/10.1371/journal.pone.0067081.
[49] S. Ohtani, A. Iwamaru, W. Deng, K. Ueda, G. Wu, G. Jayachandran, S. Kondo, E.N. Atkinson, J.D. Minna, J.A. Roth, et al., Cancer Res. 67 (2007) 6293–6303.
[50] H. Goldenberg, F.L. Crane, D.J. Morre, J. Biol. Chem. 254 (1979) 2491–2498.
[51] F.J. Rawson, A.J. Downard, K.H. Baronian, Sci. Rep. 4 (2014), https://doi.org/10.1038/srep05216.
[52] C. Kuiper, G.U. Dachs, D. Munn, M.J. Currie, B.A. Robinson, J.F. Pearson, M.C.M. Vissers, Front. Oncol. 4 (2014) 1–10.
[53] B.S. Winkler, Biochim. Biophys. Acta, Gen. Subj. 1117 (1992) 287–290.
[54] J.M. May, S. Mendiratta, K.E. Hill, R.F. Burk, J. Biol. Chem. 272 (1997) 22607–22610.
[55] B. Del Bello, E. Maellaro, L. Sugherini, A. Santucci, M. Comporti, A.F. Casini, Biochem. J. 304 (Pt 2) (1994) 385–390.
[56] W.W. Wells, D.P. Xu, Y. Yang, P.A. Rocque, J. Biol. Chem. 265 (1990) 15361–15364.
[57] E. Maellaro, B. Del Bello, L. Sugherini, M. Comporti, A.F. Casini, Methods Enzymol. 279 (1997) 30–35.
[58] J.M. May, C.E. Cobb, S. Mendiratta, K.E. Hill, R.F. Burk, J. Biol. Chem. 273 (1998) 23039–23045.
[59] A. Ito, S. Hayashi, T. Yoshida, Biochem. Biophys. Res. Commun. 101 (1981) 591–598.
[60] J.M. May, FASEB J. 13 (1999) 995–1006.
[61] H.G. Sherman, C. Jovanovic, S. Stolnik, F.J. Rawson, Anal. Chem. 90 (2018) 2780–2786.
[62] D.J.R. Lane, A. Lawen, J. Vis. Exp. (2014) 1–10.
[63] H. Pereira, J.-F. Martin, C. Joly, J.-L. Sébédio, E. Pujos-Guillot, Metabolomics 6 (2010) 207–218.
[64] R. Tautenhahn, C. Bottcher, S. Neumann, BMC Bioinf. 9 (2008) 1–16.
[65] R.A. Scheltema, A. Jankevics, R.C. Jansen, M.A. Swertz, R. Breitling, Anal. Chem. 83 (2011) 2786–2793.
[66] D.J. Creek, A. Jankevics, K.E.V. Burgess, R. Breitling, M.P. Barrett, Bioinformatics 28 (2012) 1048–1049.
[67] L.W. Sumner, A. Amberg, D. Barrett, M.H. Beale, R. Beger, C.A. Daykin, T.W.-M. Fan, O. Fiehn, R. Goodacre, J.L. Griffin, et al., Metabolomics 3 (2007) 211–221.
[68] B. Faubert, K.Y. Li, L. Cai, C.T. Hensley, J. Kim, L.G. Zacharias, C. Yang, Q.N. Do, S. Doucette, D. Burguete, et al., Cell 171 (2017) 358–371 (e9).
[69] T. Bernas, J. Dobrucki, Cytometry 47 (2002) 236–242.
[70] P. Lu, D. Ma, C. Yan, X. Gong, M. Du, Y. Shi, Proc. Natl. Acad. Sci. U. S. A. 111 (2014) 1813–1818.
[71] P.M. Herst, T. Petersen, P. Jerram, J. Baty, M.V. Berridge, Biochem. Pharmacol. 74 (11) (2007) 1587–1595.
[72] P.M. Herst, M.V. Berridge, Curr. Mol. Med. 6 (8) (2006) 895–904.
[73] E. Vlachodimitropoulou, R.J. Naftalin, P.a Sharp, Free Radic. Biol. Med. 48 (2010) 1366–1369.
[74] A.E. Del Valle, A. Del Castillo-Olivares, F. Sánchez-Jiménez, J. Márquez, I. Núñez De Castro, M.A. Medina, Protoplasma 205 (1998) 169–173.
[75] P.P. Hsu, D.M. Sabatini, Cell 134 (2008) 703–707.
[76] R.A. Gatenby, R.J. Gillies, Nat. Rev. Cancer 4 (2004) 891–899.
[77] S. Pavlides, D. Whitaker-Menezes, R. Castello-Cros, N. Flomenberg, A.K. Witkiewicz, P.G. Frank, M.C. Casimiro, C. Wang, P. Fortina, S. Addya, et al., Cell Cycle 8 (2009) 3984–4001.
[78] Y. Fu, S. Liu, S. Yin, W. Niu, W. Xiong, M. Tan, G. Li, M. Zhou, Oncotarget 8 (2017) 57813–57825.
[79] M.I. Koukourakis, D. Kalamida, A.G. Mitrakas, M. Liousia, S. Pouliliou, E. Sivridis, A. Giatromanolaki, Lab. Investig. 97 (2017) 1321–1331.
[80] C.T. Hensley, B. Faubert, Q. Yuan, N. Lev-Cohain, E. Jin, J. Kim, L. Jiang, B. Ko, R. Skelton, L. Loudat, et al., Cell 164 (2016) 681–694.
[81] S.E. Weinberg, N.S. Chandel, Nat. Chem. Biol. 11 (2015) 9–15.